scientific reports

Check for updates

OPEN

Study on failure mechanism and energy dissipation law of single fissured coal in different tectonic stress areas

Tianwei Lan[1,2]✉, Yonghao Liu[1], Fuping Wang[3], Guoqiang Wu[4], Zhu Li[3], Xiangdong Ling[3], Chuang Zhang[5], Guoqiang Liu[3] & Wei Feng[3]

To study the failure mechanism and energy dissipation law of fissured coal in different tectonic stress areas, the No.9 coal seam of the Limin coal mine was taken as the research background. The hollow inclusion stress relief method is used to measure the in-situ stress, reveal the distribution law of mine in-situ stress, and divide it into different tectonic stress areas. The UDEC numerical simulation software was used to analyze and study the failure mechanisms and energy dissipation characteristics of coal containing single fissures with different dip angles in high stress areas and stress gradient areas. The results show that: ① When in the same stress area, the stress concentration area at the end of the fissure dip angle 45° is the largest, and the macroscopic mechanical properties are the worst. The fissure dip angle is deflected from 45° to both sides, and the stress transfer effect and macroscopic mechanical properties are gradually improved. When it reaches 0° and 90°, the stress distribution of coal is the most uniform and the macroscopic mechanical properties are the strongest. With the increase of the fissure dip angle, the total energy and elastic strain energy of the system decrease first and then increase. The greater the fissure dip angle, the more severe the fissure damage inside the coal, which leads to the weakening of the total energy of the system and the strengthening of the dissipation capacity. ② When the fissure dip angle is the same, with the increase of stress level, the stress around the coal fissure in the high stress area is larger than that in the stress gradient area, and the stress concentration area at the fracture end is also larger, which is more prone to shear dilatancy and form dilatancy effect. At the same time, the total energy of the system gradually increases with the increase of the stress level, and the coal is prone to energy accumulation, which aggravates the occurrence of dynamic disasters.

Coal is a complex, heterogeneous natural geological material. Under prolonged geological action, it has many weak structural planes, such as fissures and joints. The existence of weak structures makes the fissured coal more likely to break, resulting in spalling, coal bursting, and other dynamic phenomena[1,2]. In addition, the structural planes such as joints, bedding, and fissures in coal largely determine the strength and deformation characteristics of coal, and the stress environment of coal plays a decisive role in the structure of coal and the deformation and failure of fissures in coal. Therefore, under the influence of the in-situ stress field of the mine, the higher the stress level, the more developed the fissure of the coal, and it is easy to expand and penetrate under the influence of the mining activities, thus the macroscopic instability failure occurs[3–5]. Therefore, the structural planes, such as joints and fissures in coal, are simulated by prefabricating fissures with different dip angles, and the characteristics of fissure closure, initiation, expansion, and penetration deformation of fissured coal under various stress levels are studied. At the same time, under the action of in-situ stress field, axial loading is used to simulate the influence of mining activities, and the energy evolution characteristics of fissured coal in the loading process are studied, so as to further clarify the disaster-causing mechanism of instability and failure of coal and ensure the safety of mine production.

In recent years, domestic and foreign scholars have carried out a large number of experimental and numerical simulation studies on the influence of different fissure dip angles on coal instability, and have achieved

[1]College of Mining, Liaoning Technical University, Fuxin, China. [2]Ordos Institute of Liaoning Technical University, Ordos, China. [3]Inner Mongolia Limin Coal Co, Ltd, Wuhai Energy Group, CHN Energy, Ordos, China. [4]Hongliu Coal Mine of Ningxia Coal Industry Co, LtdCHN Energy, Ningxia, China. [5]Ordos Haohua Hongqingliang Mining Co, Ltd, Beijing Haohua Energy Group, Beijing Energy Group, Ordos, China. ✉email: ltw821219@163.com

many research results. Bi et al.[6] conducted uniaxial compression tests on prefabricated fissure specimens with different dip angles to analyze the physical and energy evolution characteristics of coal during loading. Liu.[7] used a uniaxial compression test machine to load fissured coal with different dip angles and analyzed the mechanical evolution characteristics under uniaxial load conditions. Combined with industrial CT scanning, the three-dimensional visualization reconstruction of the internal fissures of the loaded coal was carried out, and the macroscopic and microscopic evolution laws of the coal fissures under different confining pressure conditions were analyzed. Shang.[8] used laboratory tests and numerical simulation to analyze the fissure and deflection state of fissures in coal with different dip angles during uniaxial compression, and compared and analyzed the fissure propagation path and stress evolution process in different loading stages, and the fissure propagation path and stress evolution process in different loading stages were compared and analyzed. Zhu et al.[9] using the PFC numerical simulation method, conducted uniaxial compression tests on coal with different fissure dip angles and types to study the energy dissipation characteristics within the coal and the influence mechanism on the impact tendency. Wang. et al.[10] explored the precursor information of coal instability and coal distribution characteristic parameters with different fissure dip angles. Based on the uniaxial loading test of coal, they analyzed the mechanical characteristics of coal and the law of fissure evolution, derived the accurate expression of the gas fissure angle, and established the mechanical model of bending fissure. The above research on the physical and mechanical properties of coal with different fissure dip angles has made great progress. However, the essence of progressive failure of coal is driven by the external energy, and the internal fissures of coal gradually close, fissure, expand, and penetrate each other, which eventually leads to macroscopic instability and failure of coal. SZECOWKA et al.[11] put forward an index of the energy accumulation ability of coal during the loading process, which is the ratio of elastic energy accumulated to the plastic energy consumed during the unloading process. Gong et al.[12,13] defined the peak strength strain energy storage index and the residual elastic energy index as the ratio of the elastic strain energy density to the dissipated strain energy density at the peak strength of the specimen and the difference between the peak elastic strain energy density and the energy density after peak failure, respectively. The above research results play an important role in clarifying the energy evolution mechanism of coal with different fissure dip angles in the process of compressive instability and failure.

Due to the physical and mechanical properties, as well as the energy evolution characteristics of coal with different fissure dip angles, domestic and foreign scholars have achieved significant results. However, there are few reports on the mechanical properties, fissure propagation evolution, and energy evolution characteristics of fissured coal in different tectonic stress areas. Based on in-situ stress measurement of the mine, this study employs UDEC7.0 (Universal Distinct Element Code 7.0) numerical simulation to analyze the deformation and failure characteristics of coal with single fissures and different dip angles in different tectonic stress areas and to determine the progressive failure process and energy evolution laws of fissured coal under different stress levels. The findings of this research will hold significant practical implications for mine mining activities and dynamic disaster prediction.

In-situ stress measurement and tectonic stress area division in coal mine

General situation of mine

The Limin coal mine is located in the southeast of the Zhuozishan coalfield, which belongs to the Wuhai Energy Company of the National Energy Group. The strike length of the mine is about 3.27 km, the dip length is about 3.30 km, and the total area is about 7.9862km^2. The design production capacity of the mine is 1.5Mt/a, and the mixed development mode of the inclined shaft is adopted. A production layout of one shaft on one side is adopted. The longwall comprehensive mechanized coal mining method is adopted, and the roof is managed by all caving methods. The mine has a monoclinic structure inclined to the southwest-west (SWW). The terrain is generally high in the south and low in the north. The elevation is generally between + 1425 ~ + 1350 m. The dip angle of the stratum is gentle, generally 5 ~ 10°, and the local cut by the fault can reach about 25°. There is little change in the occurrence form of the coal seam, and the structure is relatively complex. The mining plan and structural distribution of the Limin coal mine are shown in Fig. 1.

Hollow inclusion stress relief method measurement

Measuring point arrangement and operation process

To grasp the distribution of in-situ stress in No.9 coal seam of the Limin coal mine, in conjunction with the filed engineering conditions, two in-situ stress measuring points were arranged in No.9 coal seam, with a total of three measuring holes. The measuring point 1 is located at 3700 m in the gentle slope inclined shaft of Limin coal mine, and two measuring holes are arranged. The measuring point 2 is located in a horizontal ring yard of No.9 coal seam, and one measuring hole is arranged[14]. The drilling parameters of in-situ stress measurement points are shown in Table 1.

The operation process of in-situ stress measurement mainly includes test preparation, test drilling, hollow inclusion stress meter installation, three-dimensional stress relief, measured strain data acquisition, and result calculation and analysis[15]. The test process is shown in Fig. 2.

Measurement results and stress field characteristics analysis

The collected data are output as Excel files and Origin software is used to draw the measured strain and release distance curves. The strain-release distance curves of typical measuring points and coal-rock core inclusions are shown in Fig. 3. *A*, *B,* and *C* represent three measuring points of strain gauges on the hole wall, which are distributed at 120° intervals. ε_z is the axial strain, ε_θ is expressed as tangential strain, $\varepsilon_{45°}$ is expressed as an oblique strain of 45° with the borehole axis. $\varepsilon_{-45°}$ is expressed as an oblique strain of -45° with the borehole axis.

The analysis reveals that the strain-relief distance curve can be divided into three distinct stages. The first stage is characterized by strain fluctuation, which occurs far from the strain gauge and thus has minimal impact

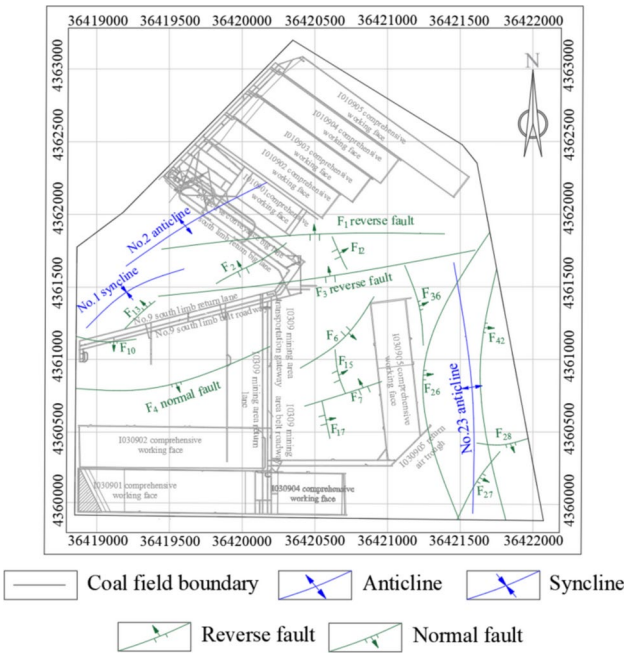

Fig. 1. Mining plan and structure distribution of Limin coal mine.

Measuring point	Measuring point position	Depth of embedment/m	Drilling depth/m	Borehole orientation/°	Dip angle of hole/°	Probe installation angle/°
No.1	No.1 hole of gentle slope inclined shaft 3700 m	296	8.75	NE185°	3	5
No.2	No.2 hole of gentle slope inclined shaft 3700 m	296	9.31	NE275°	3	0
No.3	Horizontal ring yard of No.9 coal seam	324	9.82	NE175°	4	4

Table 1. Basic parameters of in-situ stress measuring points in No.9 coal seam of Limin coal mine.

(a) Hit the test hole

(b) Installation of hollow inclusion stress meter

(c) Three-dimensional stress relief

(d) Measured strain data acquisition

Fig. 2. In-situ stress test of No.9 coal seam in Limin coal mine.

on the strain value. The second stage is known as the strain surge stage. During this phase, as the release distance increases, the rock mass surrounding the strain gauge breaks off, leading to a gradual release of three-dimensional stress. Consequently, the value of each strain gauge rises with the increasing release distance. The third stage is the strain stabilization stage. In this stage, as the release distance continues to increase, the three-dimensional stress is fully released, causing the values of each strain gauge to stabilize.

According to the plane strain theory[16]. The mine in-situ stress data are analyzed, and the analysis results are shown in Table 2.

According to the analysis Table 2, the distribution of in-situ stress in the mine is $\sigma_H > \sigma_v > \sigma_h$, it belongs to the type of strike-slip fault stress field. The maximum lateral pressure coefficient K_H is 2.19 ~ 2.63, which is greater than 1, with an average of 2.43. Therefore, the mine is dominated by horizontal tectonic stress. The maximum horizontal principal stress direction is N75.47°E ~ N85.78°E, with an average of N79.69°E.

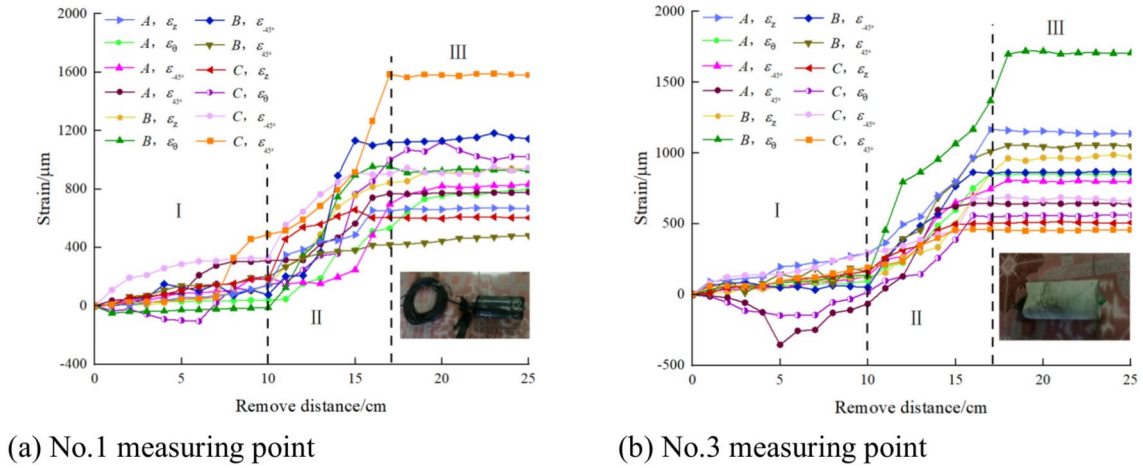

Fig. 3. Typical stress relief curve and coal-rock core inclusion in Limin coal mine.

Measuring point	Depth of embedment /m	Maximum horizontal principal stress /σ_H		Vertical stress σ_v/MPa	Minimum horizontal principal stress σ_h/MPa	Coefficient of hori-zontal pressure			Type of in-situ stress field
		Size /MPa	Direction /°			K_H	K_{av}	K_h	
No.1	296	17.9	255.47	8.19	7.77	2.19	1.57	0.95	Strike-slip fault stress field
No.2	296	20.60	265.78	8.38	7.22	2.46	1.66	0.86	
No.3	324	24.98	77.81	9.51	8.35	2.63	1.75	0.88	

Table 2. In-situ stress analysis results of No.9 coal seam in Limin coal mine.

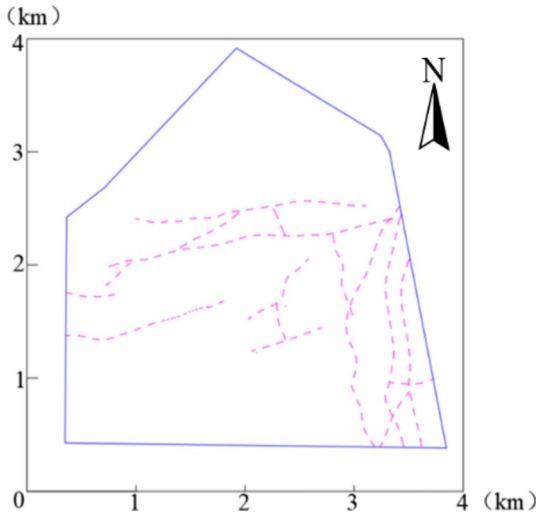

Fig. 4. Geological structure model of No.9 coal seam.

Division of mine tectonic stress area

The theory of geodynamic area is a branch of geodynamics. Through theoretical analysis, in-situ stress measurement and numerical simulation, the interaction between faults and other structures is revealed, the stress state of rock mass is determined, and the possible geological effects of engineering activities are predicted[17,18].

Application of geodynamic area method[19,20]. The fault structure of Limin coal mine is divided into two grades according to different scales, that is, the fault drop is 0 ~ 100 m and the fault drop is greater than 100 m. Based on the classification of fault structure, the geological structure model of No.9 coal seam in Limin coal mine is established. The length of the model is 4 km, the width is 4 km, and the area is 16km^2, as shown in Fig. 4.

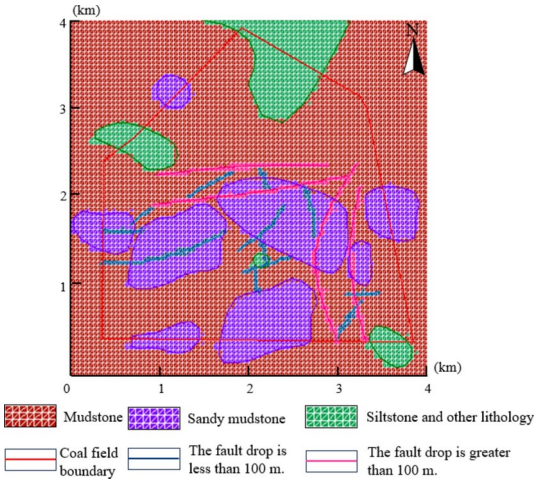

Fig. 5. Rock mass stress calculation model and lithology distribution.

Rock classification		Elastic modulus /GPa	Poisson ratio
Mudstone		11.04	0.24
Sandy mudstone		19.33	0.22
Siltstone and other lithology		24.20	0.25
Fault throw	0 ~ 100 m	15.0	0.34
	> 100 m	7.0	0.35

Table 3. No.9 coal seam roof lithology classification and parameters.

Based on the geological structure model, the self-developed 'rock mass stress state analysis system' is adopted[21]. The grid subdivision is carried out, and the information such as the distribution characteristics of roof lithology, fault structure and field boundary in the mine field is input into the calculation model, as shown in Fig. 5. The relevant parameters are shown in Table 3.

According to the measured results of in-situ stress, the in-situ stress field of Limin coal mine is mainly horizontal extrusion, which is in the regional tectonic stress field with the maximum compressive stress direction of N79.69°E. Therefore, in the calculation and analysis of rock mass stress, the maximum horizontal principal stress value should be projected to the horizontal and vertical directions for calculation.

Based on the theory of geodynamic zoning.[22] During the calculation, because the medium at the fault is non-uniform, the magnitude and direction of the stress near the fault will greatly deviate when the load is applied. Therefore, in the treatment of faults, the method of weakening the medium in the fault is used to deal with the fault, that is, the elastic modulus of the fault with a fault drop of 0 ~ 100 m is taken as 80% of the normal rock mass parameters, and the elastic modulus of the fault with a fault drop greater than 100 m is taken as 50% of the normal rock mass parameters.

According to Tables 2 and 3, mechanical parameters and boundary loads are applied to the stress calculation model to determine the rock mass stress of the No.9 coal seam in the Limin coal mine. This analysis results in the generation of contour maps for maximum principal stress, minimum principal stress, and maximum shear stress. The contour map depicting the maximum horizontal principal stress of the rock mass in the No.9 coal seam of the Limin coal mine is presented in Fig. 6.

Due to the controlling effect of fault structures on the mine's geological environment and the variation in rock properties of the coal seam roof, naturally formed high stress areas, stress gradient areas, normal stress areas, and low-stress areas can be identified within the minefield. These stress regions are detailed in Table 4, and the tectonic stress area of the rock mass is illustrated in Fig. 7.

Stress–strain curve characteristics and typical fissure distribution characteristics of fissured coal mass

Analysis of stress–strain curve characteristics of fissured coal mass

The stress–strain curve and the law of internal fissure propagation during the progressive failure process of fissured coal are shown in Fig. 8. By analyzing the progressive failure process of fissured coal in Fig. 8 (a), it is found that the failure process of coal is accompanied by the closure, initiation, expansion, and interaction of fissures, as well as the accumulation and dissipation of energy. Therefore, it has an important influence on the energy storage characteristics of coal and the occurrence of dynamic disasters under different stress conditions. According to different stress conditions, the failure process can be divided into five stages:

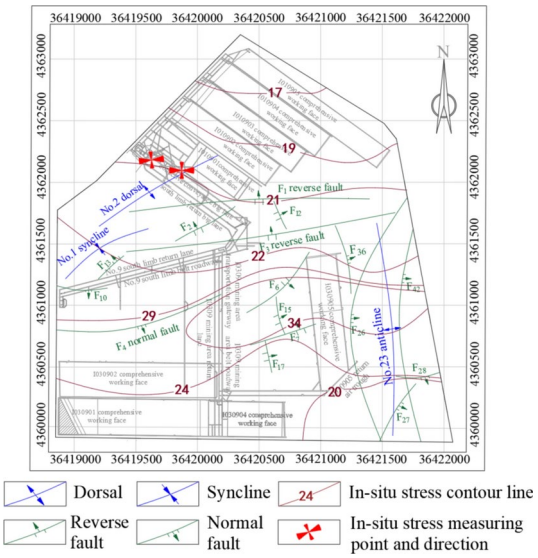

Fig. 6. The maximum horizontal stress contour map of rock mass in No.9 coal seam of Limin coal mine.

Stress concentration factor/k	Maximum horizontal principal stress /σ_H	Tectonic stress areas
$k \leq 0.8$	$14 \leq \sigma_H \leq 19$ MPa	low stress areas
$0.8 < k \leq 1.0$	$19 < \sigma_H \leq 24$ MPa	normal stress areas
$1.0 < k \leq 1.2$	$24 < \sigma_H \leq 29$ MPa	stress gradient areas
$k > 1.2$	$29 < \sigma_H \leq 34$ MPa	high stress areas

Table 4. Division of tectonic stress areas in No.9 coal seam.

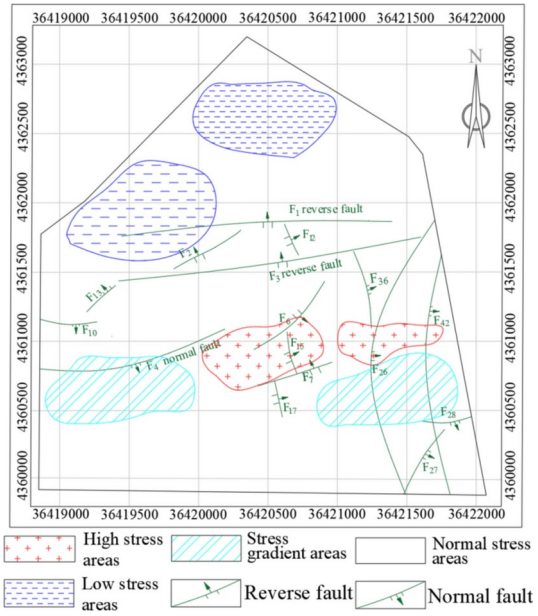

Fig. 7. Division of tectonic stress areas of No.9 coal seam rock mass in Limin coal mine.

1. Section "Introduction", fissure compaction stage. At this stage, with the increase of axial stress, the existing fissure structure inside the coal gradually closed, the relative friction phenomenon of the structural plane gradually weakened, and the internal energy of the coal gradually accumulated. The stress threshold corresponding to this stage is called fissure closure stress σ_{cc}.

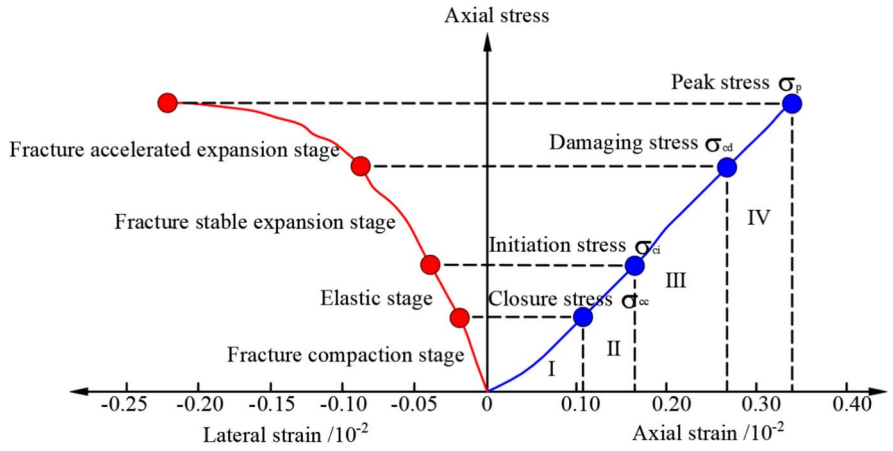

(a) Division of different stages of progressive failure process of fissured coal mass.

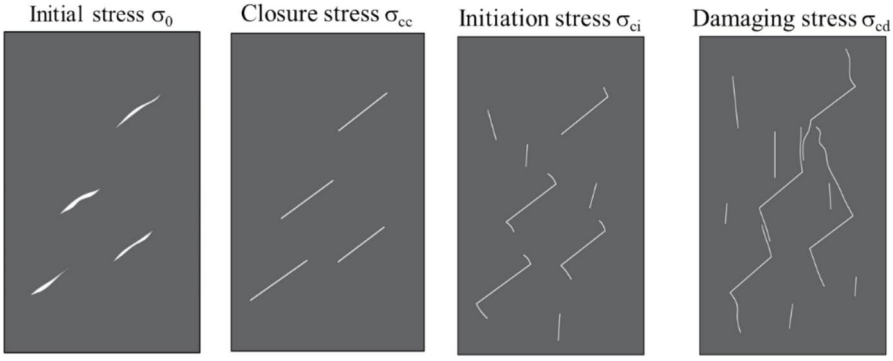

(b) The propagation law of internal fissures in coal at different stages.

Fig. 8. The stress–strain curve and internal fissure propagation law of the progressive failure process of fissured coal mass[23].

2. Section "In-situ stress measurement and tectonic stress area division in coal mine", namely the linear elastic deformation stage. When the axial stress is applied to the stress threshold σ_{cc} of the previous stage (section "Introduction"), the fissures in the coal are completely closed, and the coal enters the linear elastic deformation stage (section "In-situ stress measurement and tectonic stress area division in coal mine"). There is no obvious fissure propagation in this stage, and the total energy input is all converted into the elastic deformation energy of the coal. Therefore, the physical and mechanical parameters such as elastic modulus and Poisson ratio of coal are usually measured at this stage, and the corresponding stress threshold at this stage is called fissure initiation stress σ_{ci}.
3. Section "Stress–strain curve characteristics and typical fissure distribution characteristics of fissured coal mass", fissure stable expansion stage. When the axial stress is applied to the stress threshold σ_{ci} of the previous stage (section "In-situ stress measurement and tectonic stress area division in coal mine"), the original fissures in the coal begin to expand and gradually generate new fissures, and the progressive failure process of the coal enters the stage of stable fissure expansion (section "Stress–strain curve characteristics and typical fissure distribution characteristics of fissured coal mass"). Different degrees of damage and failure occurred on the surface and inside of the coal, and the bearing capacity decreased. The fissure propagation and the generation of new fissures in the system consume part of the energy, but the total energy of the coal is still mainly accumulated and still has a certain bearing capacity. The stress threshold corresponding to this stage is called fissure damage stress σ_{cd}.
4. Section "Analysis of failure characteristics of single fissured coal in different tectonic stress areas" fissure accelerated expansion stage. When the axial stress is applied to the stress threshold σ_{cd} of the previous stage (section "Stress–strain curve characteristics and typical fissure distribution characteristics of fissured coal mass"), the coal fissure begins to appear dilatancy failure, and the progressive failure process of the coal enters the stage of fissure accelerated expansion (section "Analysis of failure characteristics of single fissured coal in different tectonic stress areas"). The internal fissures in the coal are accelerated to expand, and the bearing capacity is destroyed. The dissipation of energy inside the coal is further intensified, and the ability of coal to accumulate energy is greatly reduced. The stress threshold corresponding to this stage is called the peak stress σ_p.
5. Post-peak crushing section. When the axial stress is applied to the stress threshold σ_p of the previous stage (section "Analysis of failure characteristics of single fissured coal in different tectonic stress areas"), the in-

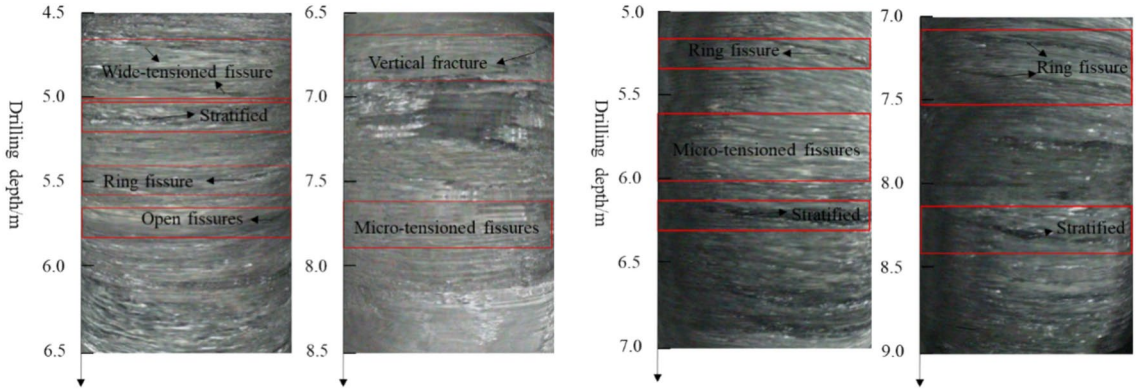

Fig. 9. Typical fissure distribution characteristics of coal.

Test type	*E*/GPa	*v*		*φ*/(°)	*c*/MPa	*R*t/MPa	*R*c/MPa
Laboratory tests	10.05	0.25		35	1.55	0.94	6.30
UDEC simulation	11.00	0.24		29	1.50	1.05	7.04

Table 5. Comparison of physical and mechanical parameters of coal. *E* represents the elastic modulus; *v* denotes Poisson ratio; *φ* denotes the friction angle; *c* denotes cohesion; *R*t represents the tensile strength; *R*c denotes compressive strength.

ternal fissures of the coal interact and form a tension fissure area or shear area, the coal is broken, and the bearing capacity is almost zero. The energy accumulated inside the coal is accelerated to release, making a sound similar to coal cannon.

Typical fissure distribution characteristics of coal

Coal fissures can be divided into closed fissures (< 1 mm), micro-tensioned fissures (1 ~ 3 mm), open fissures (3 ~ 5 mm), wide-tensioned fissures (> 5 mm), etc. according to their width[24]. Through the investigation of the structure of the fissured coal, the distribution characteristics of typical fissures in coal are shown in Fig. 9. The shallow part of the coal roadway is mainly composed of open fissures and annular fissures, and the deep part is mainly composed of closed fissures and micro-tensile fissures. Considering the influence of different stress levels, mining activities and other factors, the internal fissures of the coal undergo closure, fissure initiation, deformation expansion, and interaction forming a fissure network system, which eventually leads to the expansion and fissure of the coal.

Analysis of failure characteristics of single fissured coal in different tectonic stress areas

Establishment of numerical model of fissured coal

The uniaxial compression test of 50 mm × 100 mm complete coal was carried out using MTS815 test machine. The loading rate was 0.1 MPa/s, and the stress–strain curve during the loading process was monitored. The UDEC numerical simulation software is used to simulate the uniaxial compression loading of coal. The model adopts the Mohr–Coulomb constitutive model and opens the model large strain. The model size is 50 mm × 100 mm. The model is set to the Voronoi block model, and the parameter assignments are shown in Table 5. The bottom boundary is fixed, the left and right sides are free boundaries, and the axial stress is applied at the top. The loading rate is consistent with the uniaxial compression in the laboratory, and the stress–strain curve of the loading process is monitored in real time.

By repeatedly adjusting the assignment parameters, the simulated stress–strain curve is consistent with the experimental data. The comparison of the uniaxial compression stress–strain curve between the test and the UDEC simulation is shown in Fig. 10. The test curve is in good agreement with the numerical simulation curve. The elastic modulus, Poisson's ratio, friction angle, and Poisson's ratio applied in the simulation are similar to the numerical values obtained from the experiment. The numerical model can better invert the actual failure of the coal, and the model can be used for related research.

The UDEC7.0 numerical simulation software is used to study the deformation and failure characteristics of coal with single fissures and different dip angles in different tectonic stress areas, and the numerical model is shown in Fig. 11.

The physical and mechanical parameters of coal are shown in Table 5, and the mechanical parameters of the discontinuous structural plane are shown in Table 6. The width of the simulated fissured coal specimen is 50 mm, and the height is 100 mm. According to the measured results of in-situ stress, the relevant stress is applied, the gradient horizontal stress is applied, and the vertical displacement of the bottom is fixed. Taking the midpoint

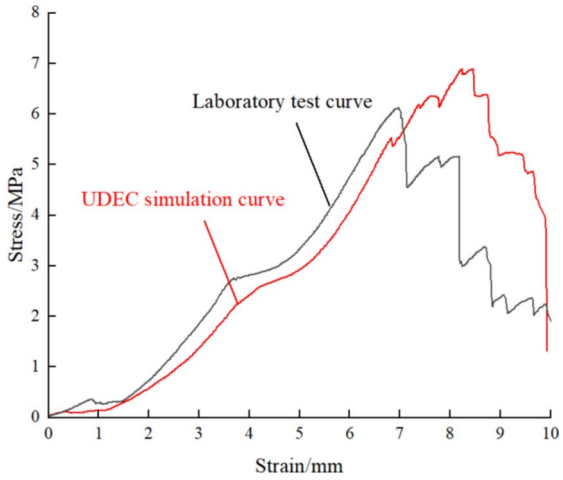

Fig. 10. The stress–strain curve of complete coal test is consistent with that of the numerical simulation.

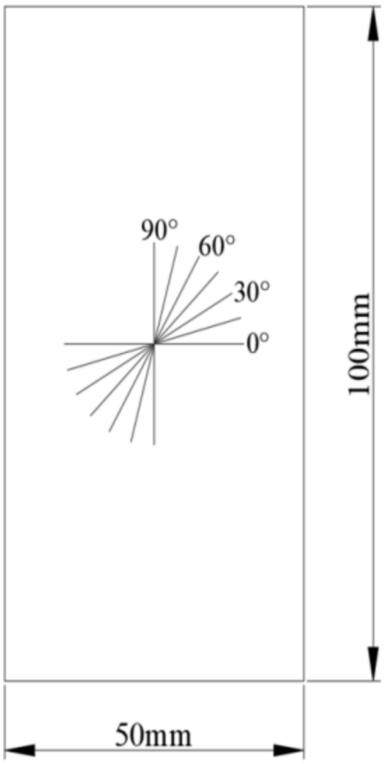

Fig. 11. Numerical model of coal with different dip angles of single fissure.

Type	K_a/MPa·mm^{-1}	K_s/ MPa·mm^{-1}	φ_j/°	C_j/MPa	R_j/MPa
Fissured coal	15.00	10.00	42	0.9	0.05

Table 6. Physical and mechanical parameters of structural plane of fissured coal. K_a is the joint normal stiffness; K_s is the joint shear stiffness; φ_j is the internal friction angle of joint; C_j is the joint cohesion; R_j is joint tensile strength. The model is carried out by the Mohr–Coulomb failure criterion.

of the model as the center of the circle, the model is constructed considering the different inclination angles of a single fissure the magnitude of the applied ground stress, and the deformation and failure characteristics of the coal fissure and its influencing factors are studied.

Progressive failure process of single fissure coal

The formation of a fissure network in coal is a random system based on stress environments, in which the principal stress interpolation is the main influencing factor. The fissure network exhibits fractal characteristics and is a superposition of multiple fissures with different dip angles. Based on the analysis of different in-situ stress characteristics and fissure characteristics, taking No.9 coal seam of Limin coal mine as an example, the failure characteristics of a single fissure with different dip angles in high stress area and stress gradient area are analyzed respectively.

In the high stress area, the fissured coal is in the accelerated expansion stage (Fig. 8(a), Section"Analysis of failure characteristics of single fissured coal in different tectonic stress areas"), and a large amount of energy is stored inside, which is prone to dynamic phenomena such as 'spalling' and 'coal burst'.

In the stress gradient area, the fissured coal is in a stable expansion stage (Fig. 8(a), Section"Stress–strain curve characteristics and typical fissure distribution characteristics of fissured coal mass"). The internal energy of the coal is continuously accumulated and the bearing capacity is decreased. Under the action of the regional in-situ stress field, it is easy to cause 'two-side deformation' and ' roof caving ' in the coal roadway.

For the normal stress area and the low stress area, the coal characteristics change little, and the fissured coal is in the stage of linear elastic change (Fig. 8(a), section"Introduction" and section "In-situ stress measurement and tectonic stress area division in coal mine"). The ability of coal volume to accumulate energy is poor, and the roadway is affected by the regional in-situ stress field. The impact is minimal and the risk of damage is the lowest. Therefore, when analyzing the deformation and failure characteristics of coal fissures under different stress levels, the coal fissures in the low stress area and the normal stress area are no longer analyzed.

Deformation and failure characteristics of single fissure coal with different dip angles

Considering the stress distribution of single fractures with different dip angles in different tectonic stress areas, the stress distribution of coal is shown in Fig. 12. The variation characteristics of single fissure coal with different dip angles in the stress gradient area are analyzed as an example.

1. When the fissure dip angle is 0° and 90°, the coal is in the fissure closure stage, and the stress state of the coal is evenly distributed without obvious stress concentration, indicating that the whole is in a stable state.
2. When the fissure dip angle is 15° and 30°, the stress concentration appears in the small area at the end of the fissure, and gradually expands to the large area in the middle along the fissure, and the stress around the fissure gradually decreases. The stress state of the fissure end is less than that of the 0° and 90° coal fissure ends.
3. When the fissure dip angle is 45°, the stress concentration phenomenon at the end of the fissure is further aggravated, and the area of the concentrated area is also larger, resulting in a large stress difference between the two ends of the fissure and the surrounding, resulting in the fissure being easy to open or move forward, and the coal is broken.
4. When the fissure dip angle is 60° and 75°, the stress around the end and middle of the fissure gradually returns to the original stress state, the area of the concentrated area is gradually smaller, and the stress on the two wings of the fissure is still symmetrically distributed.

In general, the stress concentration area at the end of the fissure dip angle 45° is the largest, the stress level is the highest, and the macroscopic mechanical properties are the worst. The fissure dip angle is deflected from 45° to both sides, and the stress transfer effect and macroscopic mechanical properties are gradually improved. When it reaches 0° and 90°, the stress distribution of coal is the most uniform and the macroscopic mechanical properties are the strongest.

The horizontal stress curve of coal with single fissures and different dip angles along the fracture length in different tectonic stress areas is shown in Fig. 13. Taking the fissure dip angle of 45° as an example, when the fissure dip angle is the same, with the increase of stress level, the stress around the coal fissure in the high stress area is larger than that in the stress gradient area, and the stress concentration area at the fissure end is also larger, which is more prone to shear dilatancy and form dilatancy effect. The two wings of the fissure propagation

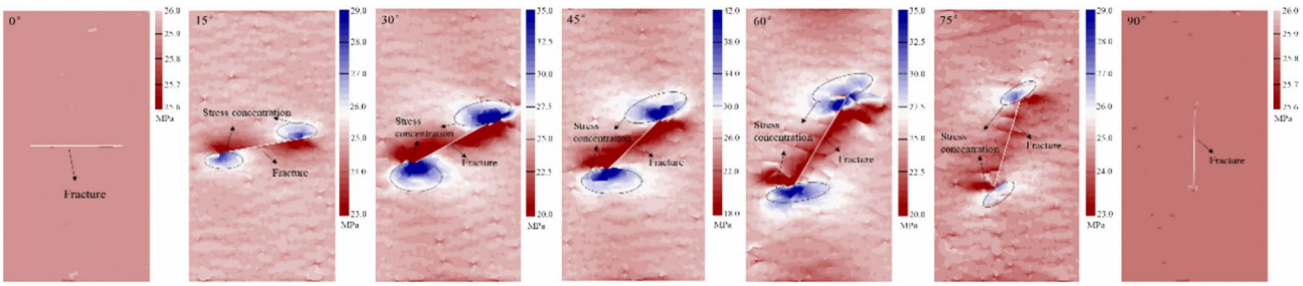

Fig. 12. Stress distribution of coal with single fissure and different dip angles in stress gradient area.

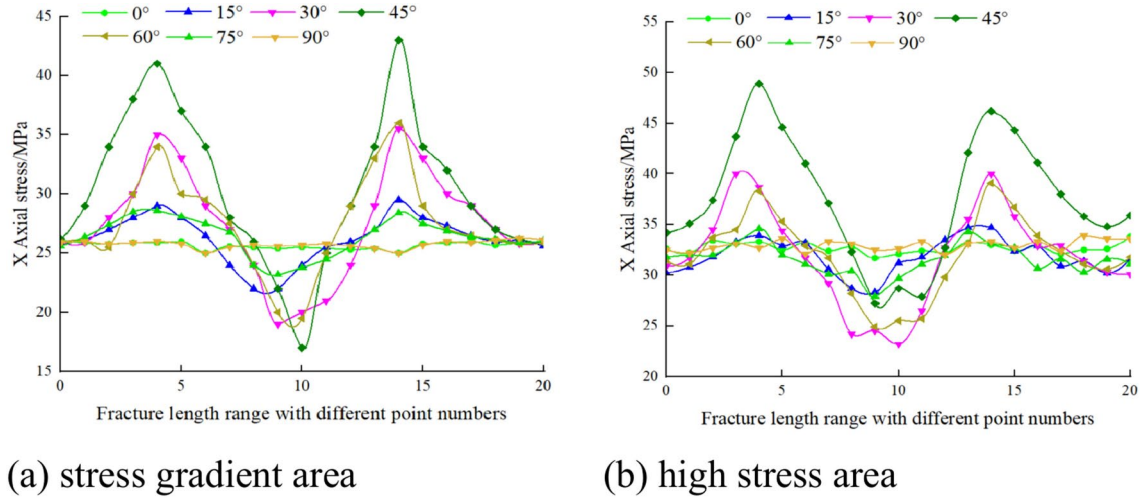

Fig. 13. The horizontal stress curves of coal with a single fissure and different dip angles in different tectonic stress areas along the fissure length direction.

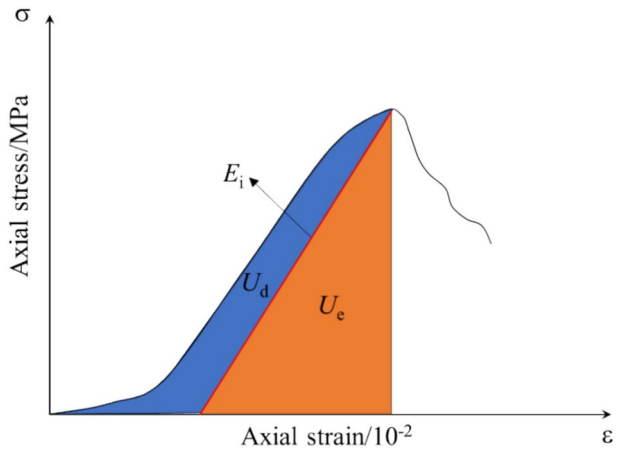

Fig. 14. The relationship between elastic strain energy U_e and dissipative strain energy U_d in the process of progressive failure of coal mass[25].

are symmetrically distributed, and the principal stress direction is asymptote extending towards the axial force direction.

Energy evolution characteristics of single fissure coal in different tectonic stress areas during the failure process

Energy calculation of fissure coal

By analyzing the characteristics of the progressive failure process of fissured coal, and the expansion of original fissures, the generation is often accompanied by the transformation of energy in the failure process of fissured coal. Throughout the entire failure process, fissured coal stores the input energy of the system as elastic strain energy. When it reaches saturation, the internal energy of the coal is released along the weak structural plane of the surface, resulting in coal crushing.

Affected by the regional tectonic stress field and mining disturbance, the fissured coal is usually accompanied by the initiation, closure, expansion, penetration and coal crushing stages of macroscopic and microscopic fissures. Therefore, the UDEC simulation software was used to axially load the fissured coal under different stress levels, and the loading rate was 0.1 MPa/s. In the process of loading and unloading, the stress–strain relationship and fissure development of fissured coal are monitored in real time. The relationship between the elastic strain energy U_e and the dissipated strain energy U_d during the loading failure process of the coal is shown in Fig. 14 [25]. The stress–strain curve can reflect the internal energy evolution process of fissured coal.

Considering the deformation and failure of fissured coal under the action of external force, it is assumed that the process has no energy exchange with the outside world, that is, it is in a closed state of the system. According

to the first law of thermodynamics, the work W of the fissure coal during the loading process is converted into the elastic strain energy U inside the coal, as shown in formula (1).

$$W{=}U = U_{\mathrm{e}} + U_{\mathrm{d}} \tag{1}$$

Therefore, for fissured coal bodies under different stress levels, different fissure distributions, and different dip angles, axial loading σ_1 does work on the coal, and lateral pressures σ_2 and σ_3 are the maximum horizontal principal stresses. The expression of each strain of energy in the coal is:

$$U = \int_0^{\varepsilon} \sigma_1 \ \mathrm{d}\varepsilon \tag{2}$$

$$Ue = \frac{1}{2Ei}\left[\sigma_1^2 + 2\sigma_3^2 - 2\mu(\sigma_3^2 + 2\sigma_1\sigma_3)\right] \tag{3}$$

$$U_{\mathrm{d}} = U - U_{\mathrm{e}} \tag{4}$$

In the formula: μ denotes poisson ratio; ε denotes the axial strain; E_i represents the unloading elastic modulus of coal, which can be replaced by the initial elastic modulus E in calculation.

Analysis of energy evolution characteristics of single fissure coal with different dip angles

The progressive failure of coal is a process of internal fissure closure, initiation, expansion, and penetration. This process is accompanied by the accumulation, dissipation and release of energy, which is a process of energy transfer and transformation[26,27]. The energy evolution characteristics of coal with single fissures and different dip angles in different tectonic stress areas are shown in Fig. 15. The total energy of the system shows an S-shaped growth trend with the increase of axial strain, which mainly undergoes three stages: Firstly, it grows at a linear constant speed, then accelerates in a concave shape, and finally slows down in a convex shape. At the same stress level, with the increase of dip angle, the total energy of the system decreases first and then increases. At the dip angle of 45°, the energy required for coal to break is the smallest. When the fracture dip angle is the same, the total energy of the system gradually increases with the increase of the stress level, and coal tends to accumulate energy, which aggravates the occurrence of mine dynamic disasters.

The fissure dip angle has a significant weakening effect on the ability of coal to store energy when it is broken under dynamic and static loads, and the phenomenon of capacity dissipation is gradually enhanced in the process of progressive failure. When the fissure dip angle is large, the fissure damage inside the coal is further aggravated, resulting in the weakening of the total energy of the system and the strengthening of the dissipation capacity.

Conclusion

1. The in-situ stress measurement was conducted using the hollow inclusion stress relief method. The maximum horizontal principal stress of No.9 coal seam rock mass in Limin coal mine was determined to be 20.6 MPa. The in-situ stress field is classified as the strike-slip fault stress field, and the maximum horizontal principal stress direction is N75.47°E ~ N85.78°E. The tectonic stress area of No.9 coal seam rock mass in Limin coal mine was divided into high stress areas, stress gradient areas, normal stress areas and low stress areas by using the self-developed 'rock mass stress state analysis system'. At the same time, it also lays a foundation for studying the failure mechanism and energy dissipation law of single-fissured coal in different tectonic stress areas.
2. Using UDEC numerical simulation software, a numerical model of coal with a single fissure and different dip angles was established, and the failure mechanism of single fissures in high stress areas and stress gradient areas was compared and studied. The results show that in the same stress area, the stress concentration area at the end of the fissure dip angle 45° is the largest, the stress level is the highest, and the macroscopic mechanical properties are the worst. The fissure dip angle is deflected from 45° to both sides, and the stress transfer effect and macroscopic mechanical properties are gradually improved. When it reaches 0° and 90°, the stress distribution of coal is the most uniform and the macroscopic mechanical properties are the strongest. When the fissure dip angle is the same, with the increase of stress level, the stress around the coal fissure in the high stress area is larger than that in the stress gradient area, and the stress concentration area at the fracture end is also larger, which is more prone to shear dilatancy and form dilatancy effect.
3. The energy dissipation law of coal with different dip angles of single fissures in high stress areas and stress gradient areas was studied through comparison. It is found that the total energy of the system shows an S-shaped growth trend with the increase of axial strain. With the increase of the fissure dip angle, the total energy and elastic strain energy of the system decrease first and then increase. The greater the fissure dip angle, the more severe the fissure damage inside the coal, which leads to the weakening of the total energy of the system and the strengthening of the dissipation capacity. When the fissure dip angle is the same, the total energy of the system gradually increases with the increase of the stress level, and the coal is prone to energy accumulation, which aggravates the occurrence of mine dynamic disasters.

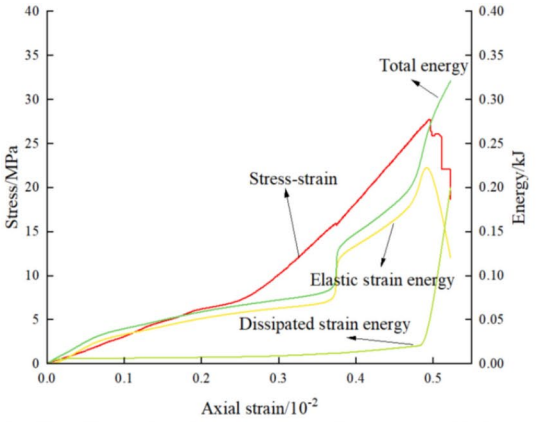

(a) The dip angle of the stress gradient area is 0° fissure coal

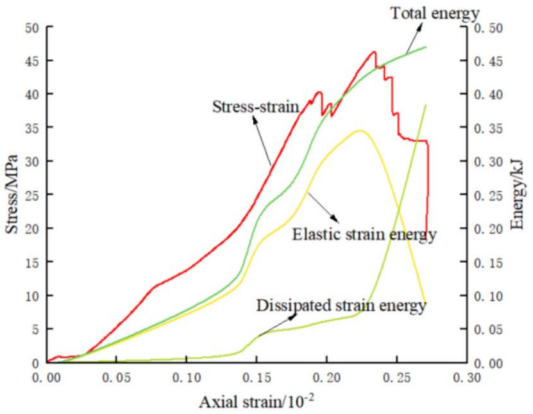

(b) The dip angle of the high stress area is 0° fissure coal

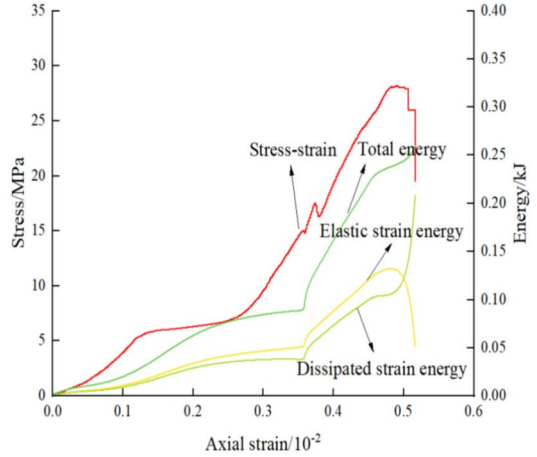

(c) The dip angle of the stress gradient area is 15° fissure coal

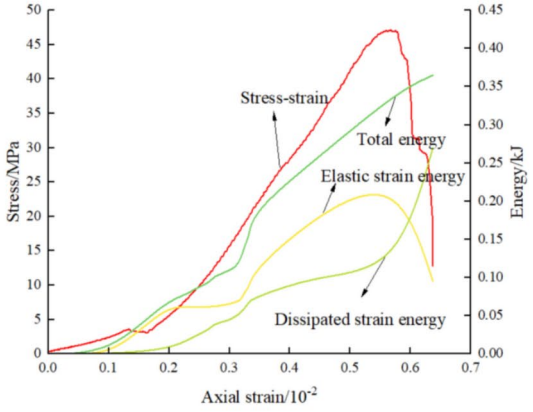

(d) The dip angle of the high stress area is 15° fissure coal

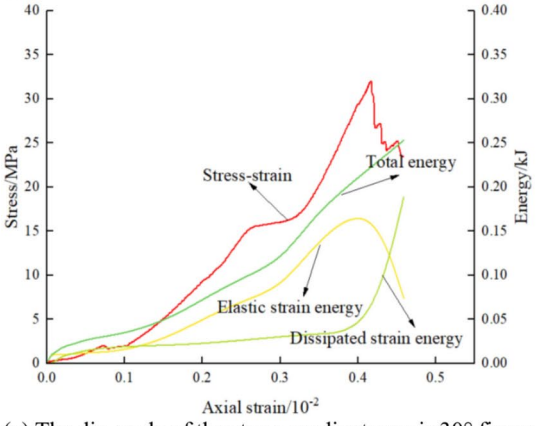

(e) The dip angle of the stress gradient area is 30° fissure coal

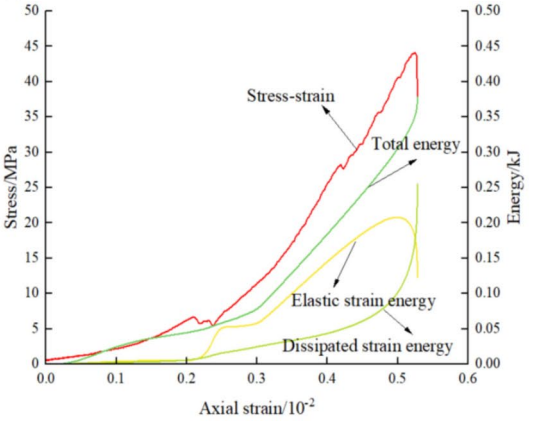

(f) The dip angle of the high stress area is 30° fissure coal

Fig. 15. Energy evolution characteristics of coal with single fissure and different dip angles in different tectonic stress areas.

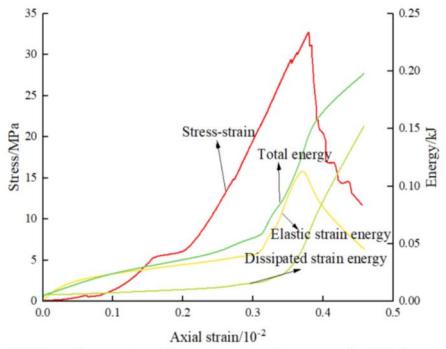

(g) The dip angle of the stress gradient area is 45° fissure coal

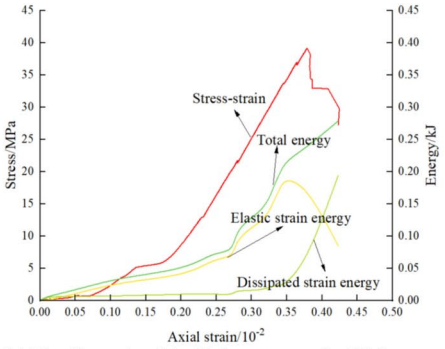

(h) The dip angle of the high stress area is 45° fissure coal

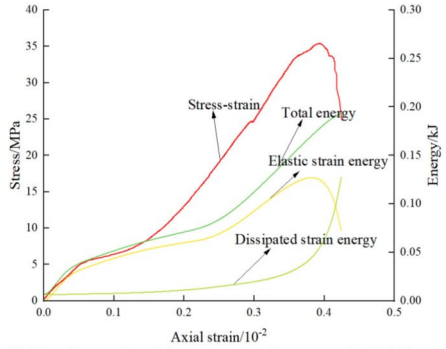

(i) The dip angle of the stress gradient area is 60° fissure coal

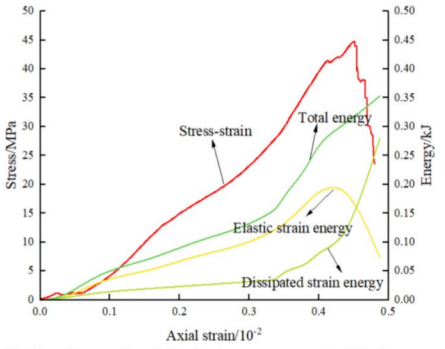

(j) The dip angle of the high stress area is 60° fissure coal

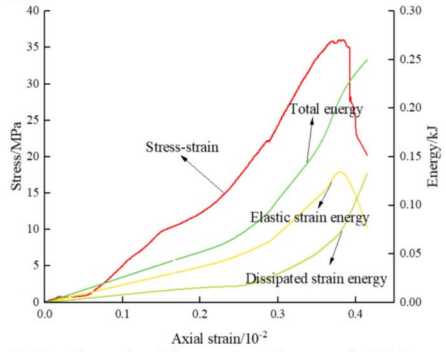

(k) The dip angle of the stress gradient area is 75° fissure coal

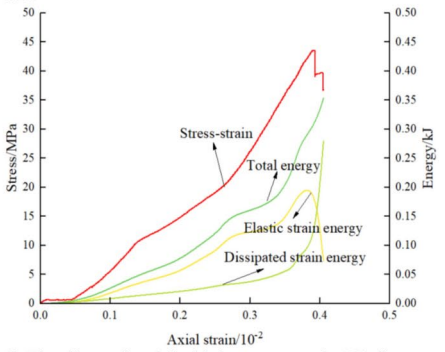

(l) The dip angle of the high stress area is 75° fissure coal

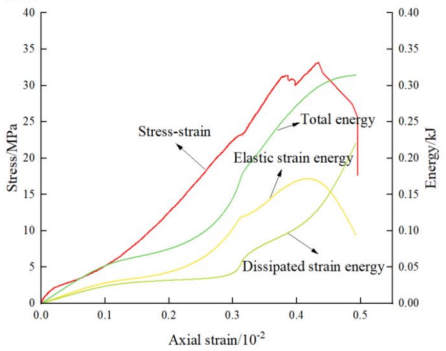

(m) The dip angle of the stress gradient area is 90° fissure coal

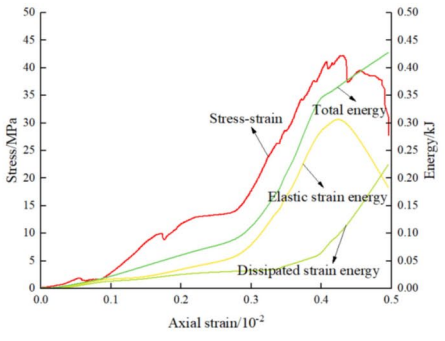

(n) The dip angle of the high stress area is 90° fissure coal

Figure 15. (continued)

Data availability

All data generated or analyzed during this study are included in this published article.

Received: 4 August 2024; Accepted: 16 December 2024
Published online: 21 February 2025

References

1. Xie, H. Research progress in deep rock mechanics and mining theory. *J. Chin. Coal. Soc.* **44**(5), 1283–1305 (2019).
2. Li, Y., Chen, L. & Wang, Y. Experimental research on pre-fissureed marble under compression. *Int. J. Solids Struct.* **42**(9/10), 2505–2516 (2005).
3. Wang, E., Wang, Z. & Wang, Y. Mechanical properties and energy evolution characteristics of fissure-bearing rocks under uniaxial compression. *Chin. J. High Pressure Phys.* **38**(1), 119–132 (2024).
4. Wang, S., Sloan, S., Shen, D., Yang, S. & Tang, C. Numerical study of failure behavior of pre-fissureed rock specimens under conventional triaxial compression. *Inter. J. Solids. Struct.* **51**(5), 1132–1148 (2014).
5. Chen, W., Yang, J., Zou, X. & Zhou, C. Research on micromechanical parameters of fissured rock mass. *Chin. J. Rock. Mech. Eng.* **27**(8), 1569–1575 (2008).
6. Bi, X. & Sun, L. Influence of fracture dip angle on coal brittleness and energy evolution. *J. Saf. Coal Mines.* **54**(9), 129–136 (2023).
7. Liu, H. Mechanical Properties and Fracture Evolution Characteristics of Coal Containing a Single Fracture and Its Application. 75-82 (Anhui University of Science and Technology, 2024).
8. Shang, R. Study on crack evolution and mechanical properties of coal with fissure under uniaxial compression. 55-58 (Anhui University of Science and Technology, 2024).
9. Zhu, Z. et al. Research on energy dissipation characteristics and coal burst tendency of fissured coal mass. *Coal. Sci. Technol.* **51**(5), 32–44 (2023).
10. Wang, L. et al. Evolution law of open fracture of coal body and instability precursor test. *J. China Univ. Mining Technol.* **53**(2), 250–263 (2024).
11. Szecowka, Z., Domzal, J., & Ozana, P. Energy index of natural bursting ability of coal. *Trans. Central. Min. Inst.* **594**, 1245–1248 (1973).
12. Gong, F., Yan, J., Li, X. & Luo, S. A peak-strength strain energy storage index for rock burst proneness of rock materials. *Inte. J. Rock. Mech. Min. Sci.* **117**, 76–89 (2019).
13. Gong, F., Wang, Y., Wang, Z., Pan, J. & Luo, S. A new criterion of coal burst proneness based on the residual elastic energy index. *Int. J. Min. Sci. Technol.* **31**(4), 553–563 (2021).
14. Dong, H. et al. Inversion and zoning characteristics of in-situ stress field in Limin Coal Mine. *Chin. Saf. Sci. J.* **33**(S2), 105–110 (2023).
15. Guo, D., Chuai, X., Zhang, T. & Guo, M. Distribution pattern and influencing factors of in-situ stress for deep levels in shoushan No.1 coal mine. *J. Chin. Coal. Soc.* **49**(5), 2360–2375 (2024).
16. Xu, Z. *A concise tutorial of elastic mechanics* (M.Higher Education Press, 2013).
17. Zhang, H. Application of geo-dynamic division method in prediction of coal and gas outburst region. *Chin. J. Rock. Mech. Eng.* **22**(4), 621–624 (2003).
18. Rong, H. et al. Characteristics of in-situ stress field and stability analysis of roadway in hongqingliang coal mine. *Coal. Geo. Explor.* **48**(5), 144–151 (2020).
19. Lan, T. et al. An evaluation method for geological dynamic environments of mines and the classification of mines subjected to rock bursts. *Coal. Geo. Explor.* **51**(2), 1–10 (2023).
20. Zhang, H. et al. Geo-dynamic division and its application in study of rock burst. *Coal. Sci. Technol.* **51**(1), 191–202 (2023).
21. Lan, T. et al. Determination of mine fault activation degree and the division of tectonic stress hazard areas. *Sci. Rep.* **14**, 12419 (2024).
22. Zhang, H. et al. *Geodynamic Division-Principle, Method, and Application* (M. Xuzhou: China University of Mining and Technology Press, 2023).
23. Peng, J., Cai, M., Rong, G., Zhou, C. & Zhao, X. Stresses for fissure closure and its application to assessing stress-induced micro-fissure damage. *Chin. J. Rock. Mech. Eng.* **34**(6), 1091–1100 (2015).
24. Li, W. et al. Deformation failure mechanism of fissured deep coal-rock mass and high-pressure grouting modification strengthening testing. *J. Chin. Coal. Soc.* **46**(3), 912–923 (2021).
25. Wang, Q. et al. Acoustic emission characteristics and energy mechanism in karst limestone failure under uniaxial and triaxle compression. *Bull. Eng. Geol. Environ.* **78**, 1427–1442 (2019).
26. Ning, J. et al. Estimation of fissure initiation and propagation thresholds of confined brittle coal specimens based on energy dissipation theory. *Rock Mech. Rock. Eng.* **51**, 119–134 (2018).
27. Huang, D., Huang, R. & Zang, Y. Experimental investigations on static loading rate effects on mechanical properties and energy mechanism of coarse crystal grain marble under uniaxial compression. *Chin. J. Rock. Mech. Eng.* **31**(2), 245–255 (2012).

Acknowledgements

The authors thank all editors and reviewers for their comments and suggestions.

Author contributions

T.L provided the original idea; Y.L wrote the main manuscript text; W.F, X.L, G.L, and Z.L provided the data in this paper; C.Z and G.W made the figures of this paper; T.L and F.W embellished this paper; Y.L is responsible for original draft writing; Y.L is responsible for review & editing.

Funding

1. Ordos city landmark innovation team ' mine geological dynamic zoning and rock burst prevention and control innovation team '(TD20240005). 2. National Natural Science Foundation of China (51,604,139).

Declarations

Competing interests

The authors declare no competing interests.

Additional information

Correspondence and requests for materials should be addressed to T.L.

Reprints and permissions information is available at www.nature.com/reprints.

Publisher's note Springer Nature remains neutral with regard to jurisdictional claims in published maps and institutional affiliations.